

Original Article

Cite this article: Fuse H, Tomita F, Yasue K, Ikoma H, Miyakawa S, Kori N, Fujisaki T, Ishimori Y, Monma M, Okumura T, and Tamaki Y. (2023) Verification of dose distribution by different material properties in intraoral mold irradiation. *Journal of Radiotherapy in Practice*. **22**(e71), 1–6. doi: [10.1017/S1460396923000286](https://doi.org/10.1017/S1460396923000286)

Received: 27 February 2023

Revised: 1 June 2023

Accepted: 26 June 2023


Keywords:

mold brachytherapy; intraoral brachytherapy; Monte Carlo simulations; TG-43

Corresponding author: Hiraku Fuse;

Email: fuseh@ipu.ac.jp

Verification of dose distribution by different material properties in intraoral mold irradiation

Hiraku Fuse¹ , Fumihiro Tomita², Kenji Yasue¹, Hideaki Ikoma³, Shin Miyakawa¹, Norikazu Kori¹, Tatsuya Fujisaki¹, Yoshiyuki Ishimori¹, Masahiko Monma¹, Toshiyuki Okumura³ and Yoshio Tamaki⁴

¹Department of Radiological Sciences, Ibaraki Prefectural University of Health Sciences, Ibaraki, Japan; ²Graduate School of Health Sciences, Department of Radiological Sciences, Ibaraki Prefectural University of Health Sciences, Ibaraki, Japan; ³Department of Radiation Technology, Ibaraki Prefectural Central Hospital, Ibaraki, Japan and ⁴Department of Radiation Oncology, Fukushima Rosai Hospital, Iwaki, Fukushima, Japan

Abstract

Background: Brachytherapy is an effective local treatment for early-stage head and neck cancers. Mold irradiation is a method in which the source is placed in the oral cavity in sites where the soft tissue is thin and an irradiation source cannot be implanted. However, dose calculations based on TG-43 may be subject to uncertainty due to the heterogeneity of tissues and materials used for the irradiation of head and neck cancers.

Materials and Methods: In this study, we investigated the basic physical properties of different materials and densities in the molds, retrospectively analysed patient plans and verified the doses of intraoral mold irradiation using a dose verification system with MC simulations specifically designed for brachytherapy, which was constructed independently.

Results and Discussion: Dose–volume histograms were obtained with a treatment planning system (TG-43) and MC simulation and revealed a non-negligible difference in coverage of high-risk clinical target volume (HR-CTV) and organ at risk (OAR) between calculations using computed tomography values and those with density changes. The underdose was 10.6%, 3.7% and 5.6% for HR-CTV, gross tumour volume and OAR, respectively, relative to the treatment plan. The calculations based on the differences in the elemental composition and density changes in TG-43, a water-based calculation algorithm, resulted in clinically significant dose differences. The validation method was used only for the cases of complex small source therapy.

Conclusion: The findings of this study can be applied to more complex cases with steeper density gradients, such as mold irradiation.

Introduction

External beam radiotherapy improves the survival rate of patients with head and neck cancers,^{1,2} but it exhibits increased adverse events due to extensive radiation exposure or localised dose increases (1–2). As the steep dose gradient characteristic of a sealed source allows the irradiated area to be localised to the tumour, brachytherapy is considered an effective topical option for treating early-stage head and neck cancers. Mold irradiation is employed to irradiate oral cavities in areas with thin soft tissues where it is difficult to implant a radiation source. In mold irradiation used for soft palate tumours, the shape of the mold is complex because it is used not only as an applicator but also as a spacer to depress the tongue. Molds are made of polymerised or thermoplastic resins, which are easy to mold to the desired dimensions. However, the density of the mold resin depends on various factors such as fabrication technique, materials used and ambient temperature.

Water-based dose calculations, based on TG-43 guidelines, are still the gold standard for brachytherapy.³ TG-43 however may cause inconsistent dose calculations for irradiation of head and neck cancers due to heterogeneity of tissues and materials.³ In contrast, dose calculations based on the Monte Carlo (MC) simulations are considered promising and the most accurate method for calculating the absorbed dose in heterogeneous materials, such as human tissues. The basic physical processes in heterogeneous human tissues and materials associated with the treatment are accurately modeled. Currently, MC simulation dose calculation engines, including EGSnrc, Geant4 and MCNP5,^{4–12} are available for several brachytherapy applications. The MC simulation can accurately calculate doses with appropriate detailed information such as atomic composition, atomic mass and electron density of tissues and materials in the calculation area. Furthermore, they can create virtual environments flexibly, allowing dose calculations even at points that are difficult to measure. In the high dose-rate (HDR) ¹⁹²Ir brachytherapy, MC- or commercial-model-based dose calculations are performed to evaluate the accuracy of the treatment planning system.^{13–15}

In this study, we verify the dose difference between TG-43 and MC simulation in dose profiles acquired with a slab phantom that reproduces the density variation of basic mold resin. Furthermore, clinical cases be retrospectively analysed to clarify the differences in dose distribution due to changes in the density of mold resin in intraoral mold irradiation.

Material and Methods

Monte Carlo simulations

The MC simulations were conducted using the egs_brachy Monte Carlo code.⁵ The egs_brachy is based on the Electron Gamma Shower National Research Council of Canada (EGSnrc) code and can simulate photons and electrons.⁵ EGSnrc can easily model complex structures using the C++ library, and many sealed small source therapy sources and applicators have been modeled.¹⁶ To perform the simulations, the MicroSelectron mHDR-v2r (Elekta AB, Stockholm, Sweden) used for treatment was modeled. The MicroSelectron mHDR-v2r geometric design and material details were adapted from a previous report,¹⁷ and the spectrum of the ¹⁹²Ir source was obtained from the National Nuclear Data Center.¹⁸ Since the absorbed dose can be approximated by collision kerma, track length estimation was employed. In all simulations, the photon and electron cut-off energies were set to 10 keV, and the statistical uncertainty was within 1% for all voxels. The absorbed dose in egs_brachy was calculated as the dose per simulated history, and Equation (1) was used to calculate the absolute dose for a given voxel x :

$$D_{absolute}^x = S_{Kmax} \frac{D_x}{S_K^{hist}} \Delta t_{max} \quad (1)$$

where S_{Kmax} is the air kerma intensity of the source at the beginning of treatment, D_x is the dose per history for a voxel x , S_K^{hist} is the air kerma intensity per history calculated for the mHDR-v2r source model and is the the maximum value at each stop time. S_K^{hist} for the MicroSelectron mHDR-v2r used in this study was 1.1909×10^{-13} Gy cm²/history, as calculated based on the report by Rogers et al.^{1,19} For commissioning the egs_brachy used in this study, the dose rate constant, radial dose function and anisotropic function reported by Granero et al. were compared with our simulation results in a water medium. They were found to be in good agreement (<2% at 0° and 180° in anisotropy function, <1% in the others).¹⁷

Comparing dose profiles using slab phantoms

The resins of mold were denture base materials, including Bruxism Sprint (BS) and GC OSTRON II (GC Inc., Tokyo, Japan). BS is thermoplastic resin, and OSTRON is polymerised resin. The elemental composition and relative electron density of the two materials are listed in Table 1.

In MC simulation, slab phantoms were prepared with the resin compositions mentioned in Table 1. Resin density varies depending on the manufacturer, ambient temperature and other environmental factors. Omnexus provides maximum and minimum density values for different types of resins.²⁰ Since the maximum and minimum densities of BS and OSTRON are unclear, dose calculations were performed for worst case scenarios of 1.5 g/cm³ and 1.0 g/cm³ as the maximum and minimum densities. Figure 1 shows the setup geometry of the slab phantom

Table 1. Elemental composition, relative electron density and physical density of material used in molds

Element	GC OSTRON II [wt%]	BS [wt%]
H	8.05	4.20
C	59.99	62.50
O	31.96	33.30
Effective atomic number	6.56	6.706
Relative electron density [g/cm ³]	1.16	1.297

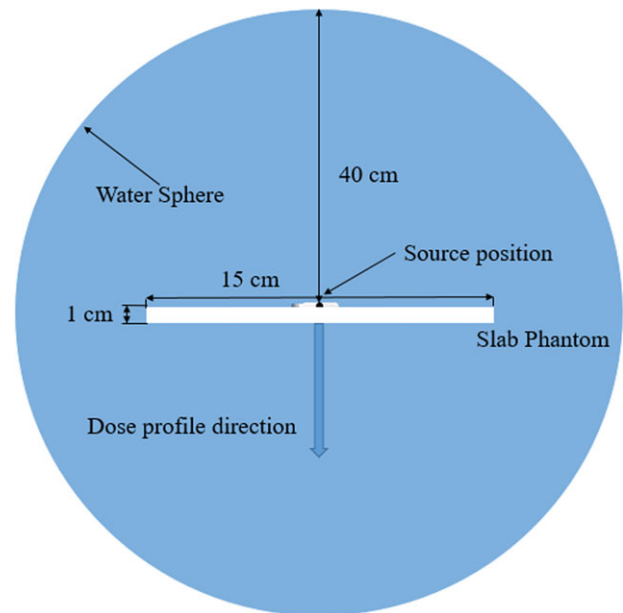


Figure 1. Geometry for calculating dose profiles using MC simulation. The source was placed in the center of a water sphere with a radius of 40 cm. The slab phantom was 1 cm thick. Dose profiles were obtained in the direction of the short axis of the source.

used in dose calculations. The calculated dose profiles were compared with TG-43 to investigate dose differences due to variation in the density of mold resins.

Dose Verification in Mold Irradiation of Soft Palate Tumours

Dose verification was performed in mold irradiation of soft palate tumours using molds made from BS and OSTRON. A patient with soft palate cancer cT2N0M0, stage II, was modelled in the validation of mold irradiation. This patient was treated with mold irradiation alone. The patient was irradiated four times with a large irradiation field, including the uvula, and three times with a reduced field (less dose to the uvula). The tumour size was 2.5 cm in the anterior–posterior direction, 2 cm in the lateral direction and 1 cm deep. The study was conducted at the authors' institutions with approval from their respective ethics committees. The mold used is shown in Fig. 2. This mold has five tubes inserted at equal intervals to create a dose distribution that fits the shape of the tumour. Three-dimensional (3D) computed tomography (CT)-based planning was performed using thin CT slices with a thickness of 1 mm in Somatom go. Open.pro (Siemens Medical Systems, Erlangen, Germany). To appropriately visualise the target, metal markers or thin copper wires were placed inside the

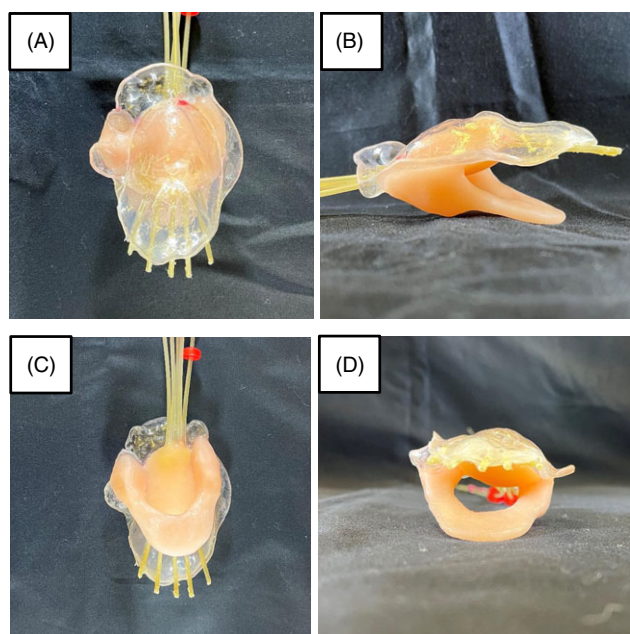


Figure 2. The images of mold applicator used for brachytherapy of soft palate cancer with A) cranial, B) right lateral, C) caudal, and D) posterior views. The clear resin is BS and the pink resin is OSTRON.

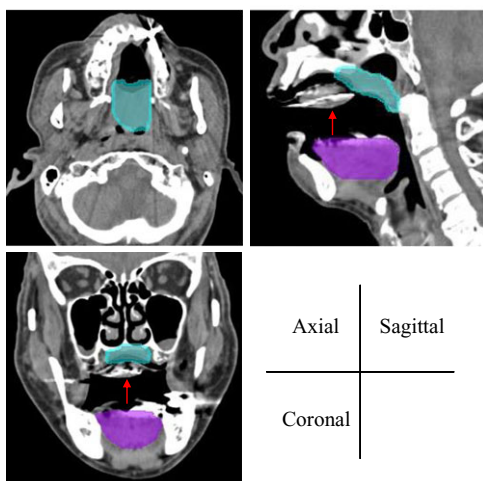


Figure 3. Three cross-sections (axial, sagittal and coronal) of the high-risk clinical target volume (HR-CTV; light blue) and organ-at-risk (OAR; purple) ROIs. The red arrows indicate the mold. High computed tomography values in the mold indicate catheters for transporting ^{192}Ir sources.

tube. A planning scan confirmed that the mold material fitted properly. The scan was repeated performed when there was an inappropriate fit due to an intervening air gap. An oncentra brachytherapy treatment planning system (TPS) version 4.5.2 (Nucletron, Elekta AB, Stockholm, Sweden) was used for the treatment planning. Figure 3 shows the ROIs (region of interest) of the high-risk clinical target volume (HR-CTV) and organ-at-risk (OAR) setups. The dose distribution was obtained by setting the dose point 120 mm from the source. The target was visualised for each slice, and the treatment plan was evaluated. Doses were prescribed based on 6 Gy per fraction and a 100% dose curve; HR-CTV was set at 3 Gy.

Patient and mold modeling in MC simulation

Anonymised patient digital imaging and communications in medicine (DICOM) data (CT data, contour data) were transferred to egs_brachy, and a voxel phantom was created in the egsphant format with a voxel size of $1\text{ mm} \times 1\text{ mm} \times 1\text{ mm}$. The density of each voxel was determined using a CT value – density calibration curve. Then, using the density of each voxel and contour information, air, fat, soft tissue and dense bone based on ICRU44²¹ were assigned to the patient body, and OSTRON II and BS compositions were applied to the mold. To investigate the change in dose distribution due to mold density changes in dose verification, the density was overridden to 1.0 g/cm^3 and 1.5 g/cm^3 without changing the composition. In this study, the MC simulation with mold density determined from CT value is defined as $\text{MC}_{\text{reference}}$. MC_{dmin} and MC_{dmax} were defined as the values calculated with MC simulation overriding the mold density to 1.0 g/cm^3 and 1.5 g/cm^3 , respectively. The dose distributions of these MCs were calculated and compared with TPS. Since the available evidence in TG-186 does not directly support $D_{\text{w,m}}$, it is preferable to report $D_{\text{m,m}}$, a conceptually well-defined quantity, as opposed to $D_{\text{w,m}}$, a theoretical quantity with no physical realisation in nonaqueous media.²² Therefore, tissue-absorbed doses were calculated in this study.

Dosimetric evaluation

DVH parameters were obtained for the TPS and all simulations using 3D Slicer.²³ To evaluate dose changes caused by the differences in the molds and dose calculation algorithms, $D_{98\%}$, $D_{90\%}$, $V_{100\%}$, $V_{150\%}$, $V_{200\%}$, and dose homogeneity index (DHI) were calculated for HR-CTV and gross tumour volume (GTV). The $D_{2\text{cc}}$ of tongue, OAR, was also calculated. DHI , a measure of the percentage of the high-dose regions within the target, was calculated using Equation (2).

$$DHI = \frac{V_{100\%} - V_{150\%}}{V_{100\%}} \quad (2)$$

Results

Figure 4 shows the dose difference and dose profile with TG-43 due to the varying density of the slab phantom. With the minimum BS and OSTRON densities, the dose difference was within 1% at all points. With the maximum densities, the dose difference for BS and OS was 1.2% and 2.9%, respectively, at 2 cm from the source center.

As shown in Fig. 5, the differences between the dose distributions using TPS (TG-43) and MC simulation were evaluated by creating a dose comparison map. It shows the differences in the dose distributions generated by each algorithm and the dose distributions for different densities in the same axial slice.

As shown in Fig. 6, the difference between the TPS (TG-43) and $\text{MC}_{\text{reference}}$ results was quantified using the DVHs of HR-CTV, GTV and OAR. The DVHs of $\text{MC}_{\text{reference}}$ were evaluated with the tissue-absorbed doses ($D_{\text{m,m}}$). The HR-CTV and GTV doses were overestimated by TPS (TG-43).

Table 2 lists the DVH parameters calculated TPS(TG-43) in water-absorbed doses ($D_{\text{w,w}}$) and MC in tissue-absorbed doses ($D_{\text{m,m}}$). Locally, the optimisation index for the prescribed dose of mold irradiation is $V_{100\%}$ and $D_{90\%}$ of HR-CTV. Herein, $V_{100\%}$ and $D_{90\%}$ of HR-CTV in $\text{MC}_{\text{reference}}$ were reduced by 10.6% and 11.7% compared to the TPS (TG-43), respectively. $D_{98\%}$, $D_{90\%}$ of

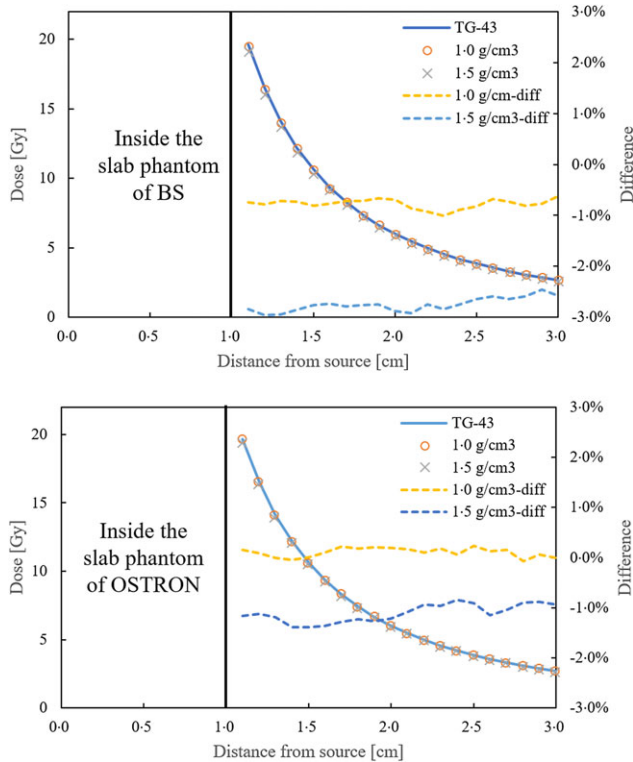


Figure 4. The dose distribution (solid line) and dose difference (dash line) with TG-43 due to the varying density of the slab phantom. The upper figure shows the calculation results by MC simulation using the slab phantom of BS, and the lower figure shows the calculation results by MC simulation using the slab phantom of OSTRON.

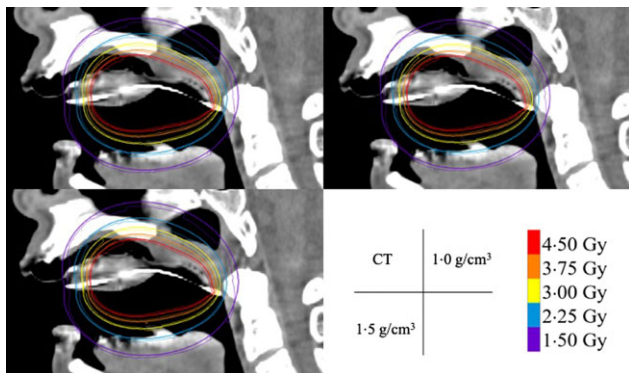


Figure 5. Tissue-absorbed dose distribution calculated using MC SIMULATION and water-absorbed it using TPS (TG-43). The thin and thick lines indicate the MC SIMULATION and TG-43 results, respectively. MC simulations were performed based on CT values (upper left) and molds overwritten to 1.0 g/cm³ (upper right) and 1.5 g/cm³ (lower left).

HR-CTV and D_{2cc} of OAR in $MC_{reference}$ differed from TPS by 0.3 Gy, 0.4 Gy and 0.1 Gy, respectively.

Of the three pattern MCs, MC_{dmax} showed the maximum deviation from TPS. The differences between MC_{dmax} and MC_{dmin} at $D_{98\%}$, $D_{90\%}$ and D_{2cc} were only <0.1 Gy and that at $V_{100\%}$ was <1%.

Discussion

As shown in Fig. 1, since the only difference between TG-43 and MC simulation geometry is the presence of a slab phantom, the

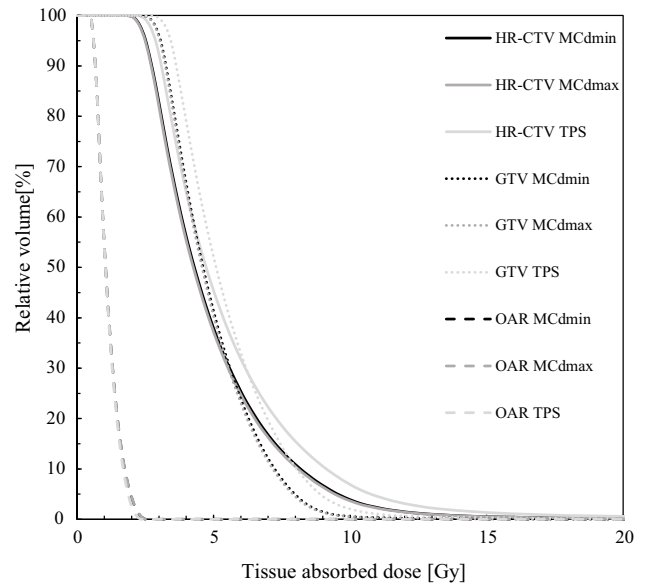


Figure 6. Dose-volume histogram (DVH) obtained using the treatment planning system (TPS; TG-43) and three patterns for Monte Carlo simulation with constant CT values and calculation with minimum and maximum densities of 1.0 and 1.5 g/cm³ overwritten to reflect density changes due to fabrication.

cause of dose difference is limited to the attenuation of this slab phantom. The dose profile shown in Fig. 4 assumes the worst case of density variation due to the environment factors during mold preparation. When the density of the slab phantom was 1.5 g/cm³, a dose difference was observed compared to TG-43. The difference is less than 3.0% despite assuming the worst-case scenario in the density difference during mold preparation. In actual mold irradiation, the dose difference of TG-43 is expected to be even smaller because the mold is thinner than 1 cm and the density is smaller than 1.5 g/cm³.

Figure 5 and Table 2 show the non-negligible difference in the doses calculated using TPS ($D_{w,w}$) and MC ($D_{m,m}$). There are significant differences in the elemental compositions and interaction cross-sections between the two algorithms because the algorithms employ different methods to determine the medium for calculating the absorbed doses. The dose in the HR-CTV was lower due to the heterogeneity. $V_{100\%}$ in Table 2 shows that the difference in the HR-CTV coverage is not negligible; the difference in D_{2cc} for OAR is also not negligible. Peppia et al. compared TG-43 and MC simulation in oral brachytherapy and observed a marked difference in the target coverage.²⁴ Similarly, in this study, there were 10.6%, 3.7% and 5.6% underdoses in HR-CTV, GTV and OAR, respectively, relative to the treatment plan. This indicates that the actual elemental composition and density changes are different from TG-43, a water-based calculation algorithm, result in clinically significant dose differences.

The treatment depth for mold irradiation was approximately 1 cm. The superimposed comparison (Fig. 5) and diametric difference of $V_{100\%}$ shows that the lack of perfect scattering conditions results in a reduced HR-CTV coverage. This is attributed to the difference in the surrounding environment of source, which directly affects the dose distribution in the tissue. For mold irradiation in the oral mucosa, the surface dose is often a limiting factor in optimising the HR-CTV coverage at a given treatment depth and may influence the dose specification method for surface mold treatments.²⁵

Table 2. $D_{98\%}$, $D_{90\%}$, D_{2cc} , $V_{100\%}$, $V_{150\%}$, $V_{200\%}$ and DHI calculated based on mold density obtained from CT value and results reflecting the mold density differences due to fabrication

Defined volume	DVH parameter	TPS (TG-43)	$D_{m,m}$					
			MC _{Reference}		MC _{dmin}		MC _{dmax}	
HR-CTV	$D_{90\%}$	3.1 Gy	2.7 Gy	(-11.7)	2.7 Gy	(-11.5)	2.7 Gy	(-12.2)
	$D_{98\%}$	2.6 Gy	2.3 Gy	(-13.2)	2.3 Gy	(-12.9)	2.3 Gy	(-13.9)
	$V_{100\%}$	92.10%	82.40%	(-10.6)	82.70%	(-10.3)	81.90%	(-11.1)
	$V_{150\%}$	54.20%	45.90%	(-15.3)	46.20%	(-14.7)	45.40%	(-16.2)
	$V_{200\%}$	31.80%	25.10%	(-20.9)	25.40%	(-20.1)	24.70%	(-22.2)
	DHI	0.4	0.4	(-7.5)	0.4	(-7.1)	0.4	(-8.2)
GTV	$D_{90\%}$	3.6 Gy	3.2 Gy	(-10.6)	3.3 Gy	(-10.3)	3.2 Gy	(-11.1)
	$D_{98\%}$	3.2 Gy	2.8 Gy	(-11.5)	2.8 Gy	(-11.2)	2.8 Gy	(-12.0)
	$V_{100\%}$	99.40%	95.70%	(-3.7)	95.90%	(-3.5)	95.40%	(-4.0)
	$V_{150\%}$	64.40%	52.50%	(-18.4)	52.90%	(-17.8)	51.90%	(-19.4)
	$V_{200\%}$	33.00%	23.60%	(-28.6)	23.90%	(-27.6)	23.10%	(-30.1)
	DHI	0.4	0.5	(-28.2)	0.4	(-27.3)	0.5	(-29.5)
OAR	D_{2cc}	1.9 Gy	2.0 Gy	(-5.6)	2.0 Gy	(-5.5)	2.0 Gy	(5.8)

The value in parentheses () indicates the percentage of difference from TPS (TG-43).

Brachytherapy using customised intraoral molds is an effective treatment for superficial oral cancer. HDR ^{192}Ir brachytherapy is a common treatment in Japan. With a dose-fractionation schedule, HDR ^{192}Ir brachytherapy with a mold has the advantage of being completed in a similar or shorter treatment period than EBRT alone and preventing accelerated repopulation.²⁶ Brachytherapy for oral cancer ranges from 20 to 40 Gy, and in Japan, it is often combined with EBRT, which ranges from 40 to 60 Gy.²⁷ When combined with EBRT, the dose must be integrated, and the dose in the oral cavity must be determined accurately. This contributes to not only curing oral cancer but also reducing adverse reactions.

Patient-specific quality assurance (QA) is performed in most facilities to validate treatment plans for complex external irradiation before treatment. Many facilities perform dosimetry with ion chamber or films in a phantom and compare the results with the dose distribution calculated using TPS. However, it is not always easy to understand how the differences affect the dose distribution for a particular patient geometry when the treatment plan is difficult to validate, as in the case of brachytherapy using molds. With the dose verification system developed here, the differences can be quantified as the target or normal tissue dose. This facilitates the interpretation of the 3D dose distribution in the evaluation of a treatment plan based on the objectives set for the plan.

The dose verification system used in this study is based on MC simulation, which allows the calculation to account for density changes. The difference between MC_{dmin} and MC_{dmax} is <0.1 Gy for $D_{98\%}$ and $D_{90\%}$ of HR-CTV, and the dose difference is <1 Gy for the entire treatment. The overridden densities are set for worst-case scenarios, and actual mold density changes will be much smaller. Therefore, the dose reduction to HR-CTV or GTV due to the density of the mold is negligible.

For OAR, differences of 5.5%–5.8% are seen in the high-dose range indicated by D_{2cc} , which can also be observed in Table 2 and Fig. 6. This difference is attributed to the heterogeneity of the oral cavity. The oral cavity is filled with mold and air, but in the TG-43 formalism, all the doses are calculated as water. MC simulation, on

the other hand, calculates doses considering their respective composition and density. Thus, the planned dose, considering the absorption of radiation by water, is lower than that calculated using MC simulation.

An important issue for patient-specific QA of treatment plans and dose distributions is the time required for such validation. In our validation, the times to start after treatment planning and finish dose calculations depend on the statistical accuracy of the MC simulations. It takes only 3 h with a statistical uncertainty of 1%. Currently, the presented validation method can only be used on demand for complex brachytherapy. In our future studies, we shall apply the proposed method to more complex cases, including mold irradiation and other cases with sharp density gradients.

Conclusion

In the irradiation of head and neck cancers using mold irradiation, dose calculations based on TG-43 are subject to uncertainty due to variations in the environment surrounding the source. Using a dose verification system based on MC simulations exclusively for brachytherapy that we constructed independently, we retrospectively analysed patient treatment plans based on the basic physical properties of the molds of different densities to validate the doses for intraoral mold irradiation.

Reference

1. Yasumoto M, Shibuya H, Hoshina M, et al. External and interstitial radiotherapy in the treatment of oropharyngeal squamous cell carcinoma. *Br J Radiol* 1995; 68: 630–635.
2. Kishino M, Shibuya H, Yoshimura R, et al. A retrospective analysis of the use of brachytherapy in relation to early-stage squamous cell carcinoma of the oropharynx and its relationship to second primary respiratory and upper digestive tract cancers. *Br J Radiol* 2007; 80: 121–125.
3. Rivard MJ, Coursey BM, DeWerd LA, et al. Update of AAPM Task Group No. 43 report: a revised AAPM protocol for brachytherapy dose calculations. *Med Phys* 2004; 31: 633–674.

4. Taylor REP, Yegin G, Rogers DW. Benchmarking BrachyDose: voxel based EGSnrc Monte Carlo calculations of TG-43 dosimetry parameters. *Med Phys* 2007; 34: 445–457.
5. Chamberland MJP, Taylor REP, Rogers DW, et al. egs_brachy: a versatile and fast Monte Carlo code for brachytherapy. *Phys Med Biol* 2016; 61: 8214–8231.
6. Afsharpour H, Landry G, D'Amours M, et al. ALGEBRA: algorithm for the heterogeneous dosimetry based on GEANT4 for brachytherapy. *Phys Med Biol* 2012; 57: 3273–3280.
7. Famulari G, Renaud MA, Poole CM, et al. RapidBrachyMCTPS: a Monte Carlo-based treatment planning system for brachytherapy applications. *Phys Med Biol* 2018; 63: article 175007.
8. Agostinelli S, Allison J, Amako K, et al. Geant4—a simulation toolkit. *Nucl Instrum Methods Phys Res Sect A* 2003; 506: 250–303.
9. Chibani O, Williamson JF. M: a sub-minute Monte Carlo dose calculation engine for prostate implants. *Med Phys* 2005; 32: 3688–3698.
10. Dolan J, Lia Z, Williamson JF. Monte Carlo and experimental dosimetry of an brachytherapy seed. *Med Phys* 2006; 33: 4675–4684.
11. Chibani O, C-M Ma C. HDRMC, an accelerated Monte Carlo dose calculator for high dose rate brachytherapy with CT-compatible applicators. *Med Phys* 2014; 41: Article 051712.
12. Team X_5 Monte Carlo, et al. MCNP—A General Monte Carlo N-Particle Transport Code. Version 5, Volume I: Overview and Theory: Los Alamos National Laboratory, Los Alamos, NM, LA-UR-03-1987, 2003.
13. Hadad K, Zohrevand M, Faghihi R, et al. Accuracy evaluation of Oncentra™ TPS in HDR brachytherapy of nasopharynx cancer using EGSnrc Monte Carlo code. *J Biomed Phys Eng* 2015; 5: 25–30.
14. Peppas V, Pappas EP, Karaiskos P, et al. Dosimetric and radiobiological comparison of TG-43 and Monte Carlo calculations in 192Ir breast brachytherapy applications. *Phys Med* 2016; 32: 1245–1251.
15. Siebert FA, Wolf S, Kóvacs G. Head and neck. 192Ir HDR brachytherapy dosimetry using a grid-based Boltzmann solver. *J Contemp Brachytherapy* 2013; 5: 232–235.
16. Buchapudi RR, Manickam R, Chandaraj V. Experimental determination of radial dose function and anisotropy function of gammamed plus 192Ir high dose rate brachytherapy source in a bounded water phantom and its comparison with egs_brachy Monte Carlo simulation. *J Med Phys* 2019; 44: 246–253.
17. Granero D, Vijande J, Ballester F, et al. Dosimetry revisited for the HDR 192Ir brachytherapy source model mHDR-v2. *Med Phys* 2011; 38: 487–494.
18. NuDat. Brookhaven National Laboratory. Decay data retrieval code. <http://www.nndc.bnl.gov/nudat3/>.
19. Rogers DWO. Inverse square corrections for FACs and WAFACs. *Appl Radiat Isot* 2019; 153: 108638.
20. Omnexus, Density of Plastics: Technical Properties. <https://omnexus.specialchem.com/polymer-properties/properties/density>.
21. ICRU Report 44, Tissue substitutes in radiation dosimetry and measurement, Int. Commission on Radiation Units and Measurements (Bethesda, MD, USA), 1989.
22. Beaulieu L, Carlsson Tedgren A, Carrier JF, et al. Report of the Task Group 186 on model-based dose calculation methods in brachytherapy beyond the TG-43 formalism: current status and recommendations for clinical implementation. *Med Phys* 2012; 39: 6208–6236.
23. Pinter C, Lasso A, Wang A, Jaffray D, Fichtinger G. SlicerRT: radiation therapy research toolkit for 3D Slicer. *Med Phys* 2012; 39: 6332–6338.
24. Peppas V, Pappas E, Major T, Takácsi-Nagy Z, Pantelis E, Papagiannis P. On the impact of improved dosimetric accuracy on head and neck high dose rate brachytherapy. *Radiother Oncol* 2016; 120: 92–97.
25. Eason L, Mason J, Cooper R, Radhakrishna G, Bownes P. Evaluation of a collapsed-cone convolution algorithm for esophagus and surface mold 192Ir brachytherapy treatment planning. *Brachytherapy* 2021; 20: 393–400.
26. Withers HR, Maciejewski B, Taylor JM, Hliniak A. Accelerated repopulation in head and neck cancer. *Front Radiat Ther Oncol* 1988; 22: 105–110.
27. Kudoh T, Ikushima H, Honda E. Shielding effect of a customized intraoral mold including lead material in high dose rate 192-Ir brachytherapy for oral cavity cancer. *J Radiat Res* 2012; 53: 130–137.